Tip Vortex Geometry of a Hovering Helicopter Rotor in Ground Effect

Jeffrey S. Light
Research Engineer
NASA Ames Research Center
Moffett Field, CA

The wide-field shadowgraph method has been used to photograph the tip vortices of a hovering helicopter rotor in ground effect. The shadowgraphs were used to obtain quantitative measurements of the rotor tip vortex geometry both in and out of ground effect. Many important phenomena are visible in the rotor wake using this method. These include the variation in descent and contraction rates of the tip vortices in ground effect, and the interaction between tip vortices in the far wake. The tip vortex geometry from the shadowgraphs is compared with the tip vortex geometry predicted using a free wake hover performance analysis. The free wake analysis accurately predicts the tip vortex geometry both in and out of ground effect. Performance data from the test is compared with the performance predicted using several methods, including the free wake analysis. All methods provided reasonable predictions of the helicopter performance in ground effect.

Notation

A	= rotor disk area, πR^2, m^2
b	= number of blades
c	= rotor blade chord, m
C_Q	= rotor torque coefficient, $Q/\rho A R V_{tip}^2$
C_{Q_0}	= profile torque coefficient
C_T	= rotor thrust coefficient. $T/\rho A V_{tip}^2$
FM	= rotor figure of merit, $C_T^{3/2}/(C_Q\sqrt{2})$
h	= distance from rotor to ground plane, m
K	= $dC_Q/dC_T^{3/2}$, slope of $C_T^{3/2}$, C_Q curve
P	= rotor power, Nm/s
Q	= rotor torque, Nm
r	= radial distance measured from rotor centerline, m
R	= rotor radius, m
T	= rotor thrust, N
V_{tip}	= rotor tip speed, ΩR, m/s
z	= axial distance measured from rotor plane, m
Ω	= rotor rotation speed, rad/s
ρ	= air density, kg/m^3
σ	= rotor solidity, bcR/A
∞	= subscript denoting out of ground effect condition

Presented at the 45th Annual Forum of the American Helicopter Society, Boston, Massachusetts, May 22-24, 1989.

Introduction

The hover performance of a helicopter is a very important design consideration since it directly affects the maximum payload of the helicopter. One method that can be used to increase the effective lifting capabilities of a helicopter is to hover close to the ground (in ground effect). Analytical and empirical methods have been developed to predict helicopter performance in ground effect (IGE) with reasonable accuracy(Refs. 1-6). Knight and Hefner (Ref. 2) developed an analytical method to predict rotor performance in ground effect, and verified it with experimental studies. They treated ground effect as a modification to the induced power of the rotor. The work of Zbrozek (Ref. 3) examined experimental results from many tests and developed an empirical method that was based on rotor height and thrust coefficient. Cheeseman and Bennett (Ref. 4) developed a simple analysis using the method of images that modeled the rotor as a source. Hayden (Ref. 6) developed a simplified empirical model from a large set of flight test data. This method was also based on a correction to the induced power. These methods all provide reasonable results, but each has certain limitations. The simple analytical methods do not account for rotor design parameters such as blade twist, chord, and sweep that may influence the hover performance in ground effect. The empirical methods are generally limited to rotor systems that are similar to those used to develop the database. Also, none of these analyses will provide information on the blade loading characteristics in ground effect.

A greater understanding of the physics of the flow is required to develop more rigorous analytical methods capable of accurately predicting the performance in ground effect for advanced rotor designs. Flow visualization can be a very important tool in understanding the physics of the flow field. Taylor (Ref. 7) examined the flow field of a hoverlng rotor in ground effect using balsa dust particles. This technique showed the overall shape of the wake, especially the radial expansion of the wake as the rotor/ground plane separation distance was decreased.

This paper describes an experimental and theoretical study of the wake geometry and performance of a helicopter rotor in ground effect. For the experimental portion of the study, a Lynx tail rotor was used to model a simple helicopter rotor in ground effect. The rotor performance was measured at many rotor/ground plane separation distances for a range of collective pitch settings. The wide-field shadowgraph method was used to obtain quantitative and qualitative information on the tip vortex geometry of the hovering rotor. The wide-field shadowgraph method is a photographic technique that detects the density variations of the tip vortices in the rotor wake (Ref. 8), allowing precise visualization of the tip vortices.

The data obtained during this test are compared to several theoretical predictions. The measured tip vortex geometry is compared to the results of a recently developed free wake hover performance analysis (Ref. 9) that models the wake of a hovering rotor in ground effect using curved vortex elements and a wake image system. The rotor performance measured during the test is compared to the predictions of the free wake analysis and predictions obtained using the methods of Cheeseman (Ref. 4) and Hayden (Ref. 6).

Test Setup

The test was conducted at the Outdoor Aerodynamic Research Facility at NASA Ames Research Center. The test apparatus consisted of a full-scale Lynx tail rotor mounted on the Tail Rotor Test Rig (TRTR) shown in Fig. 1. This four-bladed rotor had constant chord, untwisted blades with a radius of 1.105 m. More information on the tail rotor characteristics are provided in Fig. 2. The rotor shaft axis was horizontal and was located 6.07 rotor radii above the ground. The rotor was operated at tip

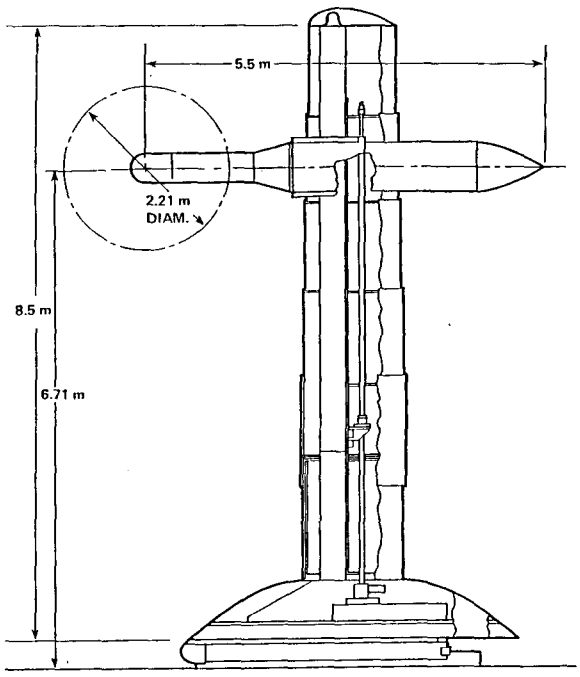

Fig. 1 Tail rotor test rig.

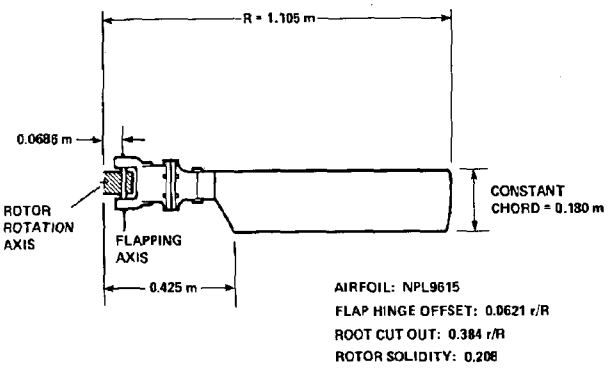

Fig. 2 Lynx tail rotor characteristics.

Mach numbers of 0.56 and 0.60, and collective pitch settings ranging from 13 deg to 17 deg. All runs were completed with ambient winds below 2.5 m/s.

A ground plane was installed in the wake of the rotor as shown in Figs. 3 and 4. The ground plane was 6.62 rotor radii in diameter, and was centered at the rotor axis. The rotor and ground plane height, approximately 6 rotor radii, were selected to minimize possible interference from the ground. Since the base of the ground plane was fixed, variations in the distance between the ground plane and the rotor were accomplished using the traversing mechanism of the TRTR. Using this traversing mechanism, the distance from the rotor to the ground plane could be varied from 0.25 to 2.5 rotor radii. All out of ground effect runs were conducted with the ground plane removed from the support stand.

The wide-field shadowgraph method was used to visualize the tip vortex geometry during the test. This method requires screens of retro-reflective material behind the flow field of interest. This material was mounted on a screen to the side of the tail rotor and on the ground plane itself (Fig. 4). These locations provided shadowgraphs which were used to determine the axial and radial coordinates of the tip vortex wake geometry. The screen to the side of the rotor was placed 6.62 R from the rotor centerline to minimize its effect on the rotor performance.

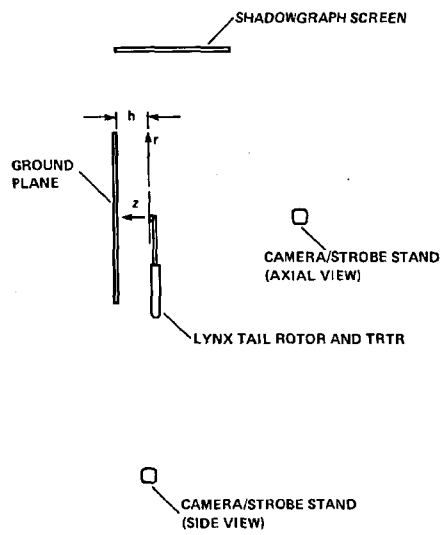

Fig. 3 Top view of test setup.

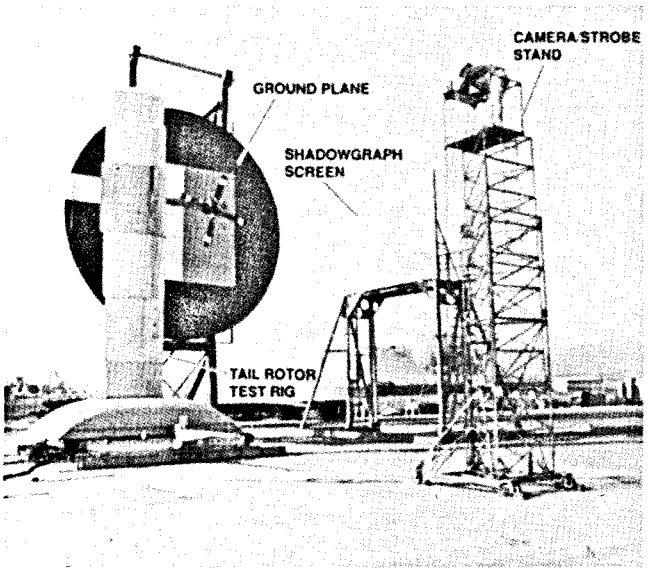

Fig. 4 Tail rotor and ground plane installation.

Rotor thrust coefficient is a major factor in determining the out of ground effect (OGE) tip vortex geometry (Refs. 10 and 11). Therefore, to examine the effect of the ground plane on the tip vortex geometry, a constant thrust was required for various rotor/ground plane separation distances. Since collective was not variable during runs, the thrust coefficient could not be varied directly. Therefore, to obtain a specified thrust coeffficient at a fixed collective, the TRTR was traversed toward or away from the ground plane until the desired thrust coefficient was achieved. The test conditions obtained using this method are shown in Table 1.

Free Wake Analysis

A free wake analysis was recently developed to calculate the performance of a hovering helicopter rotor in ground effect (Ref. 9). The analysis is based on the EHPIC (Evaluation of Hover Performance using Influence Coefficients) analysis developed by Quackenbush, *et. al.* (Ref. 12).The analysis uses a lifting surface model of the blade and curved vortex elements to model the rotor wake. A unique relaxation technique is used to calculate a free wake geometry. The effect of the ground is modeled by an image system below the rotor. Past work with this analysis out of ground effect has demonstrated its ability to predict hover performance (Ref. 13).

The free wake analysis was used to predict the performance and tip vortex geometry of the rotor in and out of ground effect. The rotor blade was modeled using three chordwise panels and 30 spanwise panels while the wake was represented by four vortex filaments trailing from each blade.

Shadowgraphs

A large database of shadowgraphs was obtained during this test over a wide range of operating conditions. Discussion of the shadowgraphs is based on the coordinate system shown in Fig. 3. The ground plane will be considered to be below the rotor, and the tip vortex axial descent will be toward the ground plane. The shadowgraphs from this test were of very high quality, with many showing the tip vortices for five turns of wake.

Table 1. Shadowgraph Run Conditions

C_T/σ	Rotor/Ground plane dist. (h/R)	Collective (Degrees)
0.102	0.78	17
0.099	0.52	16
0.093	1.92	17
0.094	0.72	16
0.095	0.32	15
0.091	OGE	17
0.090	1.20	16
0.090	0.52	15
0.090	0.26	14
0.085	OGE	16
0.084	0.96	15
0.085	0.42	14
0.080	1.54	15
0.081	0.64	14
0.080	0.34	13
0.077	OGE	15
0.077	0.46	13
0.070	OGE	14*
0.070	1.92	14
0.071	0.84	13
0.063	OGE	13*
0.064	1.90	13

***Shadowgraphs not available for these run conditions**

Tip Vortex Geometry out of Ground Effect

A sample shadowgraph obtained during testing is shown in Fig. 5. The photo is for an out of ground effect (OGE) condition with C_T/σ=0.091. The relative orientation of the blades for the shadowgraph is included in the figure. The dark section in the center of the figure was caused by the use of a different, less reflective material on that portion of the screen. Five turns of the tip vortex are clearly visible on both sides of the rotor. The shadowgraph shows the tip vortex contracting radially for the first four turns of wake. This agrees with previous research conducted on helicopter tip vortex geometry in hover (Refs. 8, 11, and 12). However, the fifth turn of wake shows significant radial expansion of the tip vortex. This expansion occurs approximately 360 deg after the tip vortex leaves the rotor blade. The expansion of the wake is accompanied by a decrease in the axial descent of the tip vortex. This is visible on both sides of the figure, but it is much more obvious on the left side. On the left side of the figure, the fourth and fifth turns of rotor wake are at about the same axial distance from the rotor. For some shadowgraphs, the fourth turn is actually further downstream than the fifth. This effect occurred consistently during the OGE runs, and was generally visible on the left of the rotor. Since this photo was taken for the out of ground effect case, this effect can not be attributed to the ground plane. This change in the tip vortex axial spacing is not currently understood.

Quantitative data were obtained from the shadowgraphs using a semi-automated data reduction technique. Up to three shadowgraphs were taken for 6 deg increments in rotor azimuth from 0 deg to 90 deg. The data reduction technique uses the outermost tip vortex location visible on each side of the rotor in each pho-

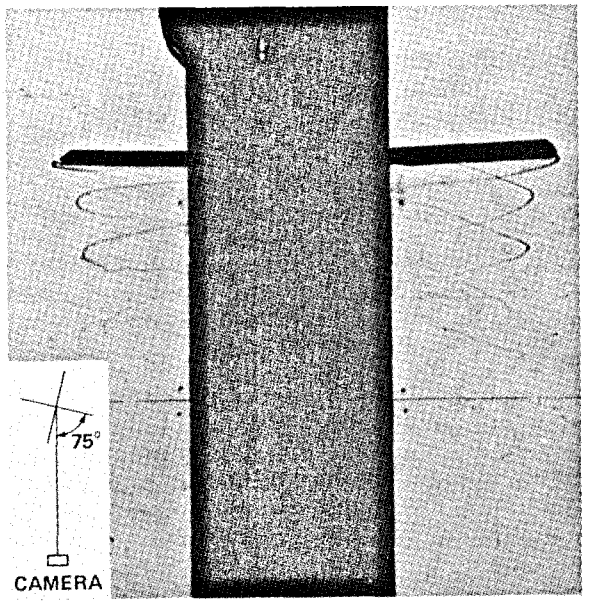

Fig. 5 Shadowgraph of tip vortices out of ground effect (C_T/σ=0.091).

tograph. For example, Fig. 5 has five data points on each side of the rotor. The radial distance from the centerline and the axial distance from the tip path plane for these points are then determined. The reduced data from the shadowgraphs out of ground effect at C_T/σ=0.091 are shown in Fig. 6.

The measured tip vortex geometry out of ground effect is compared to three predicted geometries in Fig. 6. The measured axial tip vortex location is shown in Fig. 6a. The tip vortex descent rate is constant up to the first blade passage (90 deg). At about 90 deg, the descent rate increases, and then remains constant to 270 deg. Then in the far wake, 270 deg after leaving the blade, the tip vortex location shows more variation with increasing azimuth. This shows the changes in tip vortex axial spacing that were noted in Fig. 5. The apparent scatter at the high wake azimuth angles is actually an indication of the unsteadiness of the tip vortex in the far wake.

Landgrebe's prescribed tip vortex geometry (Ref. 11) significantly underpredicts the axial descent rate of the tip vortex before the first blade passage (Fig. 6a). The Kocurek tip vortex geometry (Ref. 12) matches the measured geometry very well before and after the first blade passage. The free wake analysis predicts a higher axial descent rate before the first blade passage than is shown by the measured data. This is largely caused by insufficient resolution of the rapidly changing flow field behind the rotor blade in the tip region. Because of this, the tip vortex travels too far downward immediately following the blade (Refs. 10 and 13). The free wake analysis slightly underpredicts the tip vortex axial descent rate after the first blade passage, while the two prescribed geometries match the descent rate very closely. The variation in the far wake tip vortex location is not modeled by any of these analyses. This is expected, since all of the methods assume a distortion free, steady wake.

The measured and predicted values of the radial location of the tip vortex are shown in Fig. 6b. This shows the contraction of the tip vortex as the wake azimuth angle increases. However, at a wake azimuth angle of 270 deg, the radial location of the tip vortex also begins to vary with increasing azimuth. This corresponds to the variations in the axial tip vortex spacing.

The three wake models predict a very similar radial tip vortex location as shown in Fig. 6b. All three models show a more rapid radial contraction of the tip vortex wake than the test data. Once again, none of the methods captures the variations in the far wake.

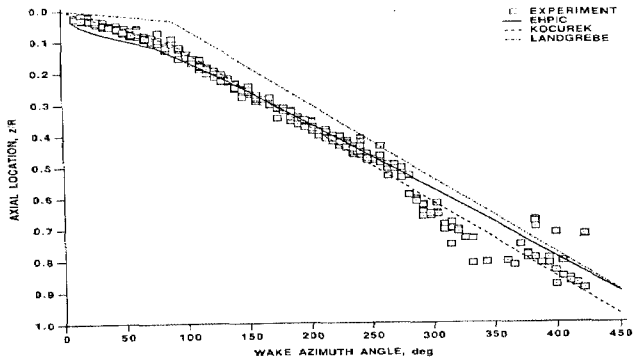

Fig. 6a Comparison of measured and predicted tip vortex axial location OGE (C_T/σ=0.091).

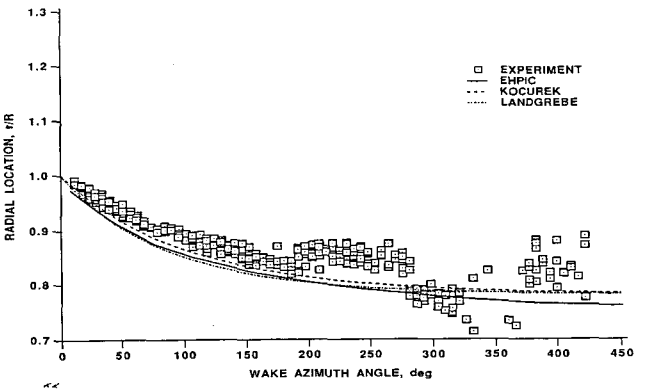

Fig. 6b Comparison of measured and predicted tip vortex radial location OGE (C_T/σ=0.091).

Tip Vortex Geometry in Ground Effect

Figure 7 shows a shadowgraph for the rotor operating in ground effect (C_T/σ=0.080 and h/R=1.54). The ground plane is visible as the dark edge of the screen at the bottom of the figure. The features visible in this shadowgraph are essentially the same as for the out of ground effect case. This figure shows the change in the tip vortex axial spacing on both sides of the rotor, as was noticed for the OGE case. This effect is so pronounced

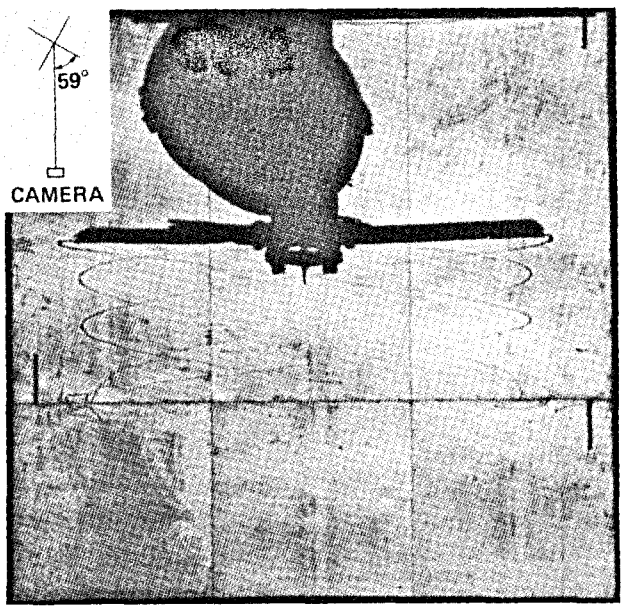

Fig. 7 Shadowgraph of tip vortices in ground effect (C_T/σ=0.080, h/R=1.54).

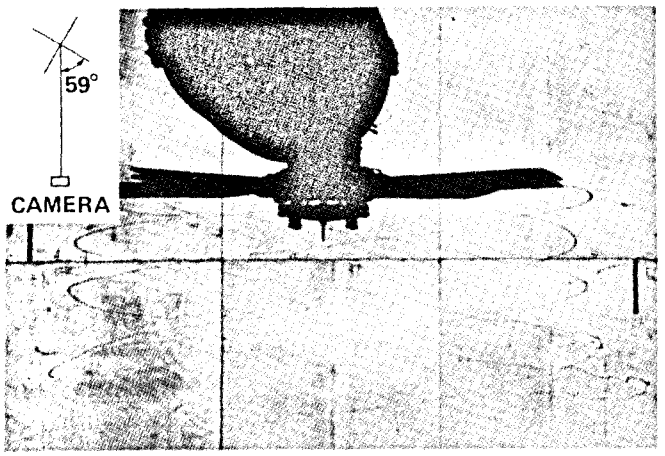

Fig. 8 Shadowgraph of tip vortices in ground effect (C_T/σ=0.084, h/R=0.96).

that the fifth turn of the wake is at the same axial location as the fourth.

Figure 8 shows a shadowgraph of the tip vortices for a smaller rotor/ground plane separation distance (C_T/σ=0.084, h/R=0.96). The tip vortex is visible for five turns of wake in this photograph. The ground plane now significantly alters the tip vortex geometry. This is most evident in the radial location of the tip vortex. The wake contracts slightly from the first turn of wake to the second, but then for each successive turn, the radial location of the tip vortex increases. The axial descent in the far wake changes in a manner similar to that noted for the OGE case. However, it is much more pronounced than in the previous shadowgraph. The fourth turn of wake is actually further downstream than the fifth turn.

Figure 9 shows the reduced tip vortex geometry data for a moderate rotor/ground plane separation distance (C_T/σ=0.071 and h/R=0.84). The axial location of the tip vortex (Fig. 9a) is very similar to the out of ground effect case. The variation in the tip vortex axial spacing is once again present, but it appears to be constrained somewhat by the ground plane.

The reduced data for the radial location of the tip vortex (Fig. 9b) shows a much more significant influence from the ground plane. This plot shows that the tip vortex trajectory contracts for only a small range of the wake. At a wake azimuth angle of about 150 deg the wake starts expanding. This is in sharp contrast to the OGE tip vortex geometry that contracts till far in the

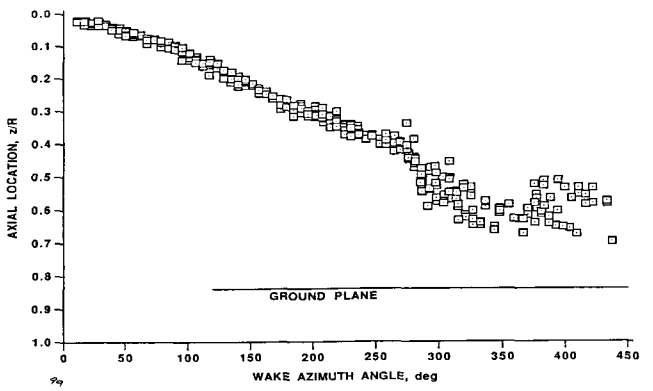

Fig. 9a. Axial location of tip vortex in ground effect (C_T/σ=0.071, h/R=0.84).

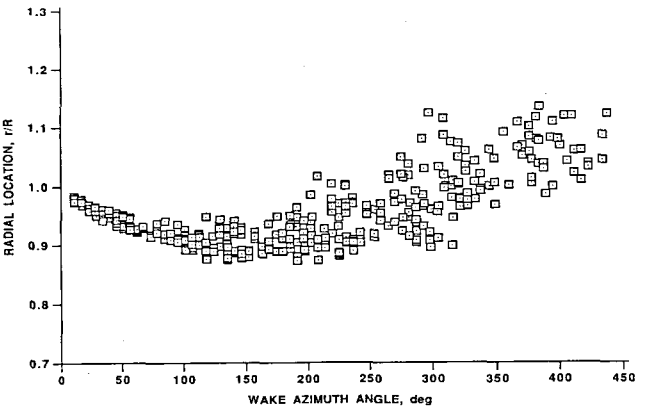

Fig. 9b Radial location of tip vortex in ground effect (C_T/σ=0.071, h/R=0.84).

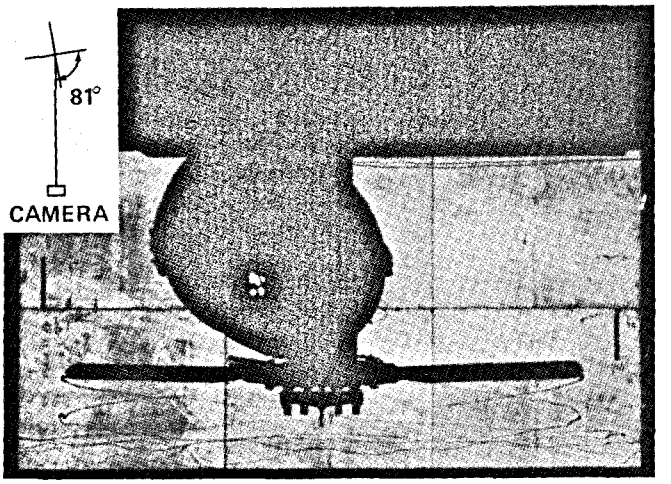

Fig. 10 Shadowgraph of tip vortices in ground effect (C_T/σ=0.095, h/R=0.32).

wake. This radial expansion was also shown in the flow visualization work of Taylor (Ref. 7). The radial data in Fig. 9b also show more apparent scatter in the far wake than was evident in the axial data shown in Fig. 9a. This suggests that the rotor wake is more unsteady in the radial direction than in the axial direction. This unsteadiness is much more noticeable for the in ground effect runs than it was for the out of ground effect runs.

Figure 10 shows a shadowgraph for the rotor very close to the ground plane (C_T/σ = 0.095, h/R=0.32). The maximum descent of the tip vortex and the tip vortex descent rate for this run condition are very obviously affected by the ground plane. Unfortunately, the screen width limits the extent of the radial wake expansion that is visible. Note that the tip vortices are still well defined for approximately four turns of wake.

The reduced tip vortex geometry data for a rotor/ground plane separation of 0.32 R is shown in Fig. 11. The axial location of the tip vortex is shown in Fig. 11a. There is no change in the axial tip vortex descent rate at the first blade passage as was evident for out of ground effect data (Fig. 6a) and in ground effect data at the larger ground plane separation (Fig. 9a). Also, the axial descent rate essentially reaches zero very near the ground plane. The axial location of the tip vortex does not show the variations in spacing evident in other shadowgraphs. This is

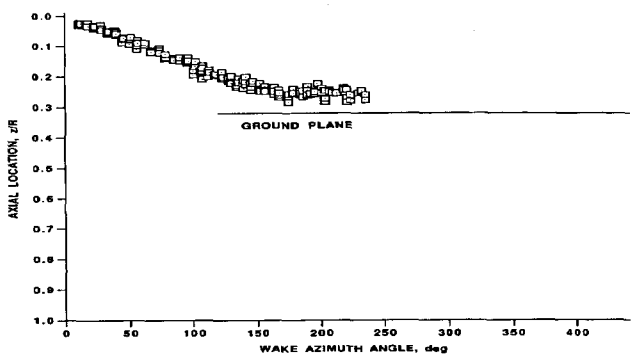

Fig. 11a Axial location of tip vortex in ground effect (C_T/σ=0.095, h/R=0.32).

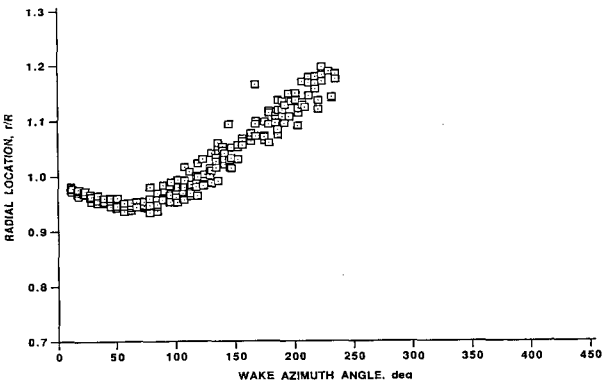

Fig. 11b Radial location of tip vortex in ground effect (C_T/σ=0.095, h/R=0.32).

because the outermost tip vortex location was not visible at large enough wake azimuth angles for the distortion to be evident. The radial location of the tip vortex is shown in Fig. 11b. This shows a slight contraction of the tip vortex, and then expansion at a faster rate than was evident for the larger ground plane distance (*i.e.* Fig. 9b). The abrupt end in the data at r/R=1.2 is caused by the screen size limitation discussed above.

As stated earlier, the thrust coefficient is a major factor influencing the tip vortex geometry for a helicopter rotor hovering out of ground effect. Therefore, to examine the effect of the ground plane on the tip vortex geometry, the thrust coefficient must be held constant. Figure 12 shows comparisons between the tip vortex geometry for variations in rotor/ground plane separation at C_T/σ=0.095. The experimental data, as represented by fitted curves (Fig. 12a), show that the ground plane has very

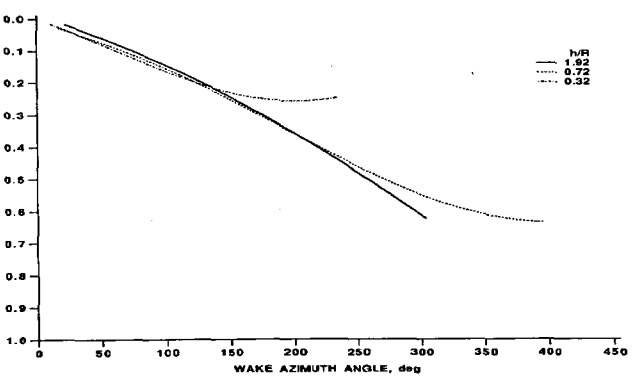

Fig. 12a Effect of rotor/ground plane separation on axial tip vortex geometry(C_T/σ=0.095).

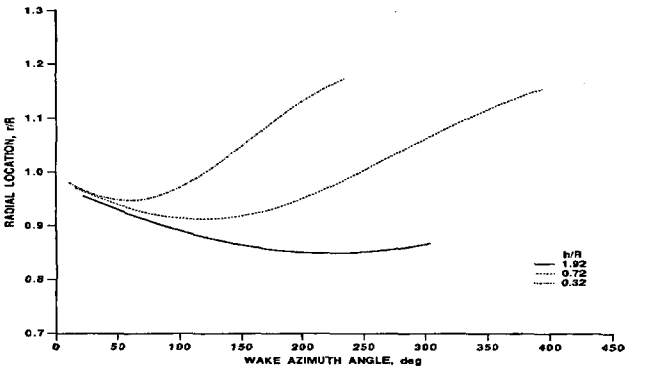

Fig. 12b Effect of rotor/ground plane separation on radial tip vortex geometry (C_T/σ=0.095) .

little effect on the tip vortex axial location in the near wake. The initial axial descent rate is essentially the same for the three different rotor/ground plane separation distances. However, there is a significant effect on the location of the tip vortex as it approaches the ground plane. Data acquired for the smaller h/R show the decrease in axial descent rate that is caused by the presence of the ground plane. This effect is not apparent for h/R=1.92, largely because the tip vortices are not visible close to the ground plane.

The rotor/ground plane separation distance has a much greater influence on the tip vortex radial location (Fig. 12b), even at ground plane distances that showed no influence on the axial location. The figure shows that the tip vortex at each h/R has a similar initial contraction rate. However, the smaller separation distance between the rotor and ground plane causes the tip vortex expansion to begin sooner, and the expansion occurs at a faster rate. The radial contraction reaches a maximum at approximately 30 percent of the rotor/ground plane separation distance, and then the tip vortex wake expands radially.

Wake Geometry Correlation in Ground Effect

Predicted and measured tip vortex geometry are compared in Fig. 13 for C_T/σ=0.090 with the rotor close to the ground plane (h/R=0.52). This figure shows the significant effect of the ground plane on the measured tip vortex geometry. The initial axial tip vortex location (Fig. 13a) is overpredicted by the analysis, which was also noted for the OGE case. The decrease in axial descent rate for larger wake azimuth angles (*i.e.*, closer to the ground plane) is modeled correctly by the free wake analysis. The predicted radial location of the tip vortex (Fig. 13b)

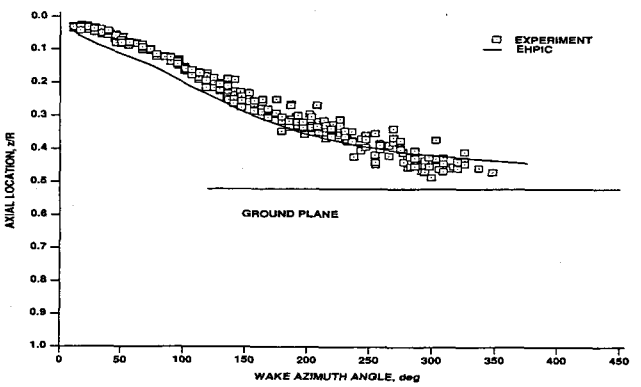

Fig. 13a Comparison of measured and predicted tip vortex axial location in ground effect (C_T/σ=0.090, h/R=0.52).

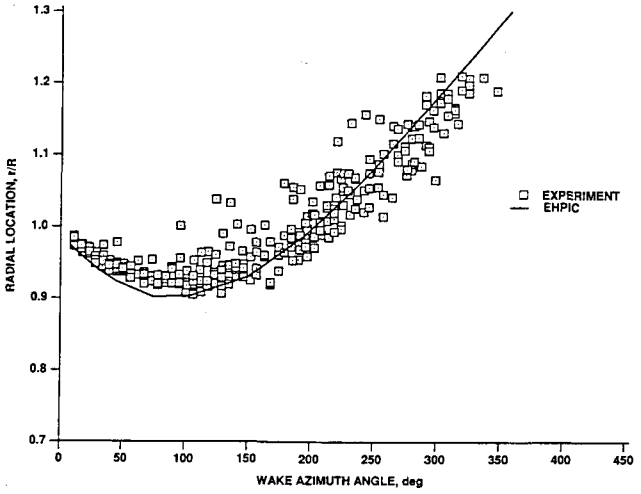

Fig. 13b Comparison of measured and predicted tip vortex radial location in ground effect (C_T/σ=0.090, h/R=0.52).

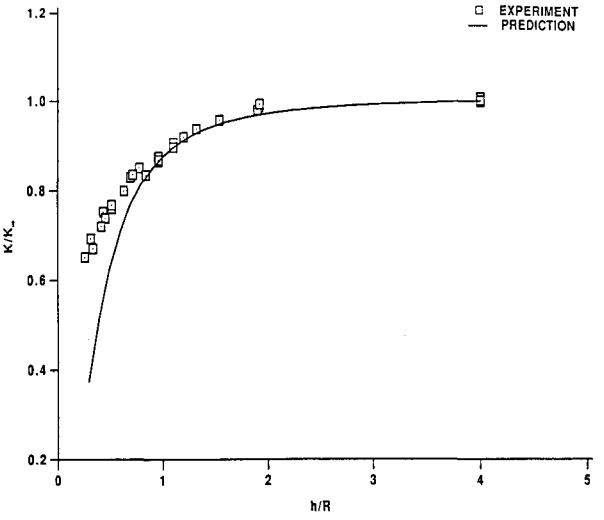

Fig. 15 Comparison of measured and predicted K/K_∞ factor

reaches maximum contraction at an earlier azimuth angle than the shadowgraph data. After the contraction, the predicted and measured geometries are very much the same.

Overall, the free wake analysis models the tip vortex geometry very well. It captures both the decrease in axial descent rate and the radial contraction/expansion caused by the ground plane with excellent accuracy.

Performance Correlations

Performance measurements were also made during testing of the rotor. For a constant collective, the ratio of the measured rotor thrust IGE to the thrust OGE plotted as a function of the rotor distance from the ground plane is shown in Fig. 14. The figure shows the averaged data obtained from each run condition. Correlation with these data was performed using three techniques.

The first technique is based on the method of Cheeseman and Bennett (Ref. 4). This is a simple analytical technique based on the method of images. Using their results, the thrust augmentation (at constant power) for a hovering rotor in ground effect is determined solely by the rotor/ground plane separation distance:

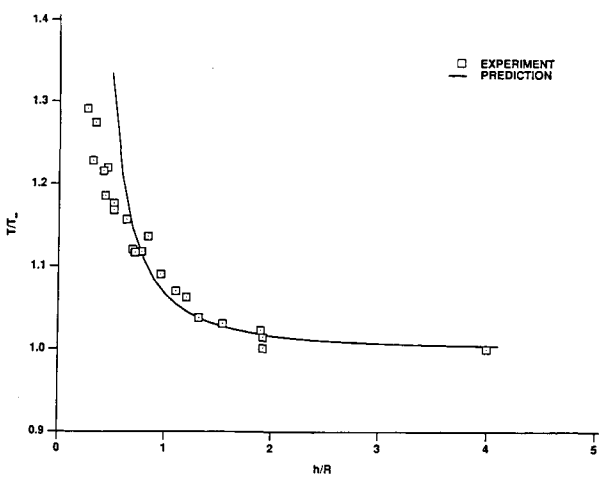

Fig. 14 Comparison of measured and predicted thrust in ground effect (Cheeseman Method).

The comparison between this prediction and the data obtained during the test is shown in Fig. 14. The OGE data are plotted at

$$\frac{T}{T_\infty} = \frac{1}{1 - \frac{R^2}{16\,h^2}}$$

h/R=4 even though there was no ground plane present during those runs. The prediction and theory agree fairly well, except at very small separation distances (h/R). This limitation was acknowledged in the original development of the method. While providing a very simple method to determine thrust augmentation, this method is limited since it does not take into account the characteristics of the rotor blade (*e.g.*, twist, planform), or operating conditions.

A second method used to predict hover performance in ground effect was the empirical method developed by Hayden (Ref. 6). This method is based on a large number of tests of helicopters hovering in ground effect. The method applies a correction factor (K/K_∞) to modify the induced power required in ground effect as shown by:

Hayden developed the following expression for K/K_∞ based

$$C_Q = C_{Q_0} + \left(\frac{K}{K_\infty}\right) K_\infty C_T^{\frac{3}{2}}$$

on a curve fit of the experimental data:

$$\frac{K}{K_\infty} = \frac{1}{0.9926 + 0.15176\left(\frac{1}{\frac{h}{R}}\right)^2}$$

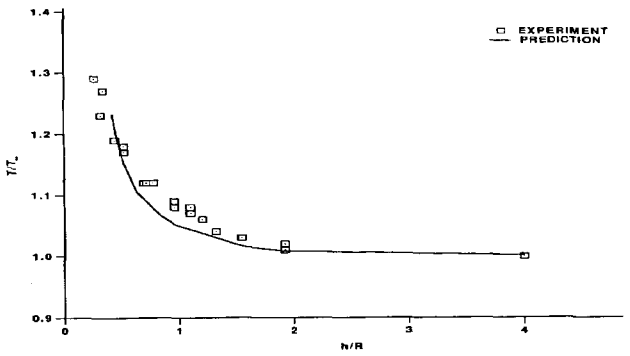

Fig. 16 Comparison of measured and predicted thrust in ground effect (EHPIC).

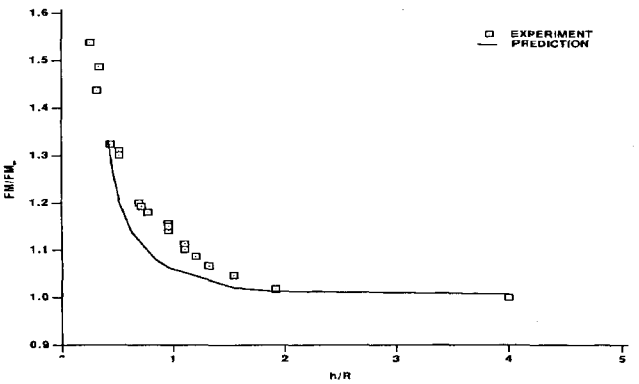

Fig. 18 Comparison of measured and predicted figure of merit in ground effect (EHPIC).

Using the performance measured during the test, K/K_∞ values were derived. These are compared with the Hayden results in Fig. 15. These data also agree well with the experimental results over a fairly small range. At small separation distances ($h/R<0.8$), this method predicts significantly lower K/K_∞ values. This would result in a lower predicted power than was actually measured. This may be caused in part by the dissimilarities between the Hayden database and the present test. Hayden's database consisted of flight test of actual helicopters rather than isolated rotor testing. Thus, his data includes corrections for tail rotor power, drive train losses, etc. This method, like that of Cheeseman and Bennett, is limited since prior knowledge of the rotorcraft OGE performance is required to determine the in ground effect performance.

The EHPIC free wake analysis was also used to predict the performance of the rotor in ground effect. The following performance plots are all shown for a constant collective as dictated by the EHPIC convergence method. The thrust augmentation vs. rotor/ground plane separation is shown in Fig. 16. The predictions and data are both shown for C_T/σ (OGE) in the range of 0.0155 to 0.0190. The predicted thrust increase is somewhat lower than the experimentally measured results. Examination of the tip vortex geometries provides no explanation for this difference in thrust. One possible explanation for the difference may lie in the treatment of the inboard vortex by the free wake analysis. In order to improve convergence, the free wake analysis fixes the location of the inboard vortex. Therefore, the recirculation in the inboard region of the rotor wake in ground effect is not modeled, and this may contribute to the lower predicted thrust.

The ratio of the IGE power to the OGE power vs. rotor/ground plane separation is shown in Figure 17. The experimental results show a small decrease in power for smaller ground plane separation distances. However, the power prediction from the free wake analysis indicates a small increase in the power. This increase in total power is caused by an increase In the calculated induced power for decreasing rotor/ground plane distances. One must keep in mind that the free wake analysis is modeling an inherently unsteady process using a steady analysis. This limitation of the analysis may be affecting the results shown here.

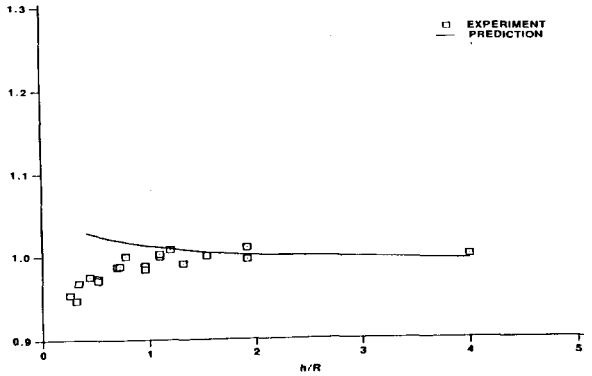

Fig. 17 Comparison of measured and predicted power in ground effect (EHPIC).

The ratio of the IGE figure of merit to the OGE figure of merit is plotted against the rotor/ground plane separation distance in Figure 18. The predicted figure of merit is close to the experimental values for the upper and lower h/R. However, the predicted value is significantly off in the midrange of rotor/ground plane separation distance. This is a result of the errors noted for the thrust and power in the previous figures.

The performance correlations completed for this work show that for the configuration tested, all three methods have the capability to predict the rotor hover performance in ground effect to a reasonable degree. However, each method has limitations that demonstrate the potential for improvement in this area.

Conclusions

This investigation examined the tip vortex geometry and performance for a helicopter rotor in and out of ground effect. The tip vortex geometry in ground effect was found to be quite different from the geometry for the out of ground effect case.

1. The axial descent of the tip vortices is significantly decreased very close to the ground plane. The radial geometry of the tip vortex contracts for a short period, and then expands rapidly. The descent rate and radial contraction/expansion are mainly functions of the rotor/ground plane separation distance.
2. The tip vortex geometry was predicted using a free wake analysis. The free wake tip vortex geometry predicted by EHPIC agreed very well with the measured geometry for a wide range of rotor/ground plane separation distances.
3. The rotor performance predicted using three methods were all in close agreement with the experimental results. The simple methods predicted the performance as accurately as the free wake analysis, and did not require as much time and computer costs. However, the free wake analysis provides a more rigorous treatment of the physics of the rotorcraft hovering in ground effect. The benefits of this capability may become more apparent as rotor designs are examined that are significantly different from designs that were used to develop the previous analytical and empirical ground effect performance prediction methods.

References

[1]Betz, A., "The Ground Effect on Lifting Propellers," NACA TM 836, Aug 1932.

[2]Knight, M., and Hefner, R., "Analysis of Ground Effect on the Lifting Airscrew," NACA TN 835, Dec 1941.

[3]Zbrozek, J., "Ground Effect on the Lifting Rotor," ARC R&M 2347, Jul 1947.

[4]Cheeseman, I., and Bennett, W., "The Effect of the Ground on a Helicopter Rotor in Forward Flight," ARC R&M 3021, Sep 1955.

[5]Fradenburgh, E., "The Helicopter and the Ground Effect Machine," *Journal of the American Helicopter Society,* Vol. 5, (4), 1960.

[6]Hayden, J., "The Effect of the Ground on Helicopter Hovering Power Required," American Helicopter Society 32nd Annual Forum, Washington, D.C., May 1976.

[7]Taylor, M., "A Balsa-Dust Technique for Airflow Visualization and its Application to Flow Through Model Helicopter Rotors in Static Thrust," NACA TN 2220, Nov 1950.

[8]Norman, T., and Light, J., "Rotor Tip Vortex Geometry Measurements Using the Wide-field Shadowgraph Technique," *Journal of the American Helicopter Society*, Vol. 32, (2), Apr 1987.

[9]Quackenbush, T., and Wachspress, D., "Enhancements to a New Free Wake Hover Analysis," NASA CR 177523, Apr 1989.

[10]Landgrebe, A., "The Wake Geometry of a Hovering Rotor and Its Influence on Rotor Performance," *Journal of the American Helicopter Society*, Vol. 17, (4), Oct 1972.

[11]Kocurek, J., and Tangler, J., "A Prescribed Wake Lifting Surface Hover Performance Analysis," *Journal of the American Helicopter Society*, Vol. 22, (1), Jan 1977.

[12]Quackenbush, T., Bliss, D., Wachspress, D., and Ong, C., "Free Wake Analysis of Hover Performance Using a New Influence Coefficient Method," NASA CR 4150, 1988.

[13]Felker, F., Quackenbush, T., Bliss, D., and Light, J., "Comparisons of Predicted and Measured Rotor Performance in Hover Using a New Free Wake Analysis," American Helicopter Society 44th Annual Forum, Washington, D.C., Jun 1988.

[14]Gessow, A., and Meyers, G. C. Jr., *Aerodynamics of the Helicopter*, Frederick Ungar Publishing Co., NY, 1952.

[15]Johnson, W., *Helicopter Theory*, Princeton University Press, NJ, 1980.

[16]Prouty, R., "Ground Effect and the Helicopter -A Summary," AIAA, AHS, and ASEE Aircraft Design Systems and Operations Meeting, Colorado Springs, CO, Oct 1985.